

# Game-theoretical mapping of fundamental brain functions based on lesion deficits in acute stroke

**Caroline Malherbe,<sup>1,2,\*</sup> Bastian Cheng,<sup>2,\*</sup> Alina Königsberg,<sup>2</sup> Tae-Hee Cho,<sup>3</sup> Martin Ebinger,<sup>4,5</sup> Matthias Endres,<sup>6,7</sup> Jochen B. Fiebach,<sup>4</sup> Jens Fiehler,<sup>8</sup> Ivana Galinovic,<sup>4</sup> Josep Puig,<sup>9</sup> Vincent Thijs,<sup>10</sup> Robin Lemmens,<sup>11,12</sup> Keith W. Muir,<sup>13</sup> Norbert Nighoghossian,<sup>14</sup> Salvador Pedraza,<sup>9</sup> Claus Z. Simonsen,<sup>15</sup> Anke Wouters,<sup>11,12</sup> Christian Gerloff,<sup>2</sup> Claus C. Hilgetag<sup>1,16</sup> and Götz Thomalla<sup>2</sup>**

\* These authors contributed equally to this work.

Lesion analysis is a fundamental and classical approach for inferring the causal contributions of brain regions to brain function. However, many studies have been limited by the shortcomings of methodology or clinical data. Aiming to overcome these limitations, we here use an objective multivariate approach based on game theory, Multi-perturbation Shapley value Analysis, in conjunction with data from a large cohort of 394 acute stroke patients, to derive causal contributions of brain regions to four principal functional components of the widely used National Institutes of Health Stroke Score measure. The analysis was based on a high-resolution parcellation of the brain into 294 grey and white matter regions. Through initial lesion symptom mapping for identifying all potential candidate regions and repeated iterations of the game-theoretical approach to remove non-significant contributions, the analysis derived the smallest sets of regions contributing to each of the four principal functional components as well as functional interactions among the regions. Specifically, the factor 'language and consciousness' was related to contributions of cortical regions in the left hemisphere, including the prefrontal gyrus, the middle frontal gyrus, the ventromedial putamen and the inferior frontal gyrus. Right and left motor functions were associated with contributions of the left and right dorsolateral putamen and the posterior limb of the internal capsule, correspondingly. Moreover, the superior corona radiata and the paracentral lobe of the right hemisphere as well as the right caudal area 23 of the cingulate gyrus were mainly related to left motor function, while the prefrontal gyrus, the external capsule and the sagittal stratum fasciculi of the left hemisphere contributed to right motor function.

- 1 University Medical Center Hamburg-Eppendorf, Institute of Computational Neuroscience, Hamburg, Germany
- 2 Neurology, University Medical Center Hamburg-Eppendorf, Hamburg, Germany
- 3 Neurology, Université Claude Bernard Lyon 1, Lyon, France
- 4 Centrum für Schlaganfallforschung Berlin (CSB), Charité, Universitätsmedizin Berlin, Berlin, Germany
- 5 Medical Park Berlin Humboldtmühle, 13507 Berlin, Germany
- 6 Department of Neurology, Charité – Universitätsmedizin Berlin, Berlin, Germany
- 7 Center for Stroke Research Berlin, Charité – Universitätsmedizin Berlin, Berlin, Germany
- 8 Department of Diagnostic and Interventional Neuroradiology, University Medical Center Hamburg-Eppendorf, Hamburg, Germany
- 9 Department of Radiology, Institut de Diagnostic per la Image (IDI), Hospital Dr Josep Trueta, Institut d'Investigació Biomèdica de Girona (IDIBGI), Girona, Spain
- 10 Stroke, The Florey Institute of Neuroscience and Mental Health, Melbourne, VIC, Australia
- 11 Neurology, UZ Leuven, Leuven, Belgium
- 12 VIB, Center for Brain & Disease Research, Laboratory of Neurobiology, Leuven, Belgium
- 13 Institute of Neuroscience & Psychology, University of Glasgow, Glasgow, UK

Received February 08, 2021. Revised May 21, 2021. Accepted July 01, 2021. Advance Access publication September 2, 2021

© The Author(s) (2021). Published by Oxford University Press on behalf of the Guarantors of Brain.

This is an Open Access article distributed under the terms of the Creative Commons Attribution License (<https://creativecommons.org/licenses/by/4.0/>), which permits unrestricted reuse, distribution, and reproduction in any medium, provided the original work is properly cited.

14 Department of Stroke Medicine, Université Claude Bernard Lyon 1, Lyon, France

15 Department of Neurology, Aarhus University Hospital, Aarhus N, Denmark

16 Department of Health Sciences, Boston University, Boston, MA, USA

Correspondence to: Caroline Malherbe, PhD

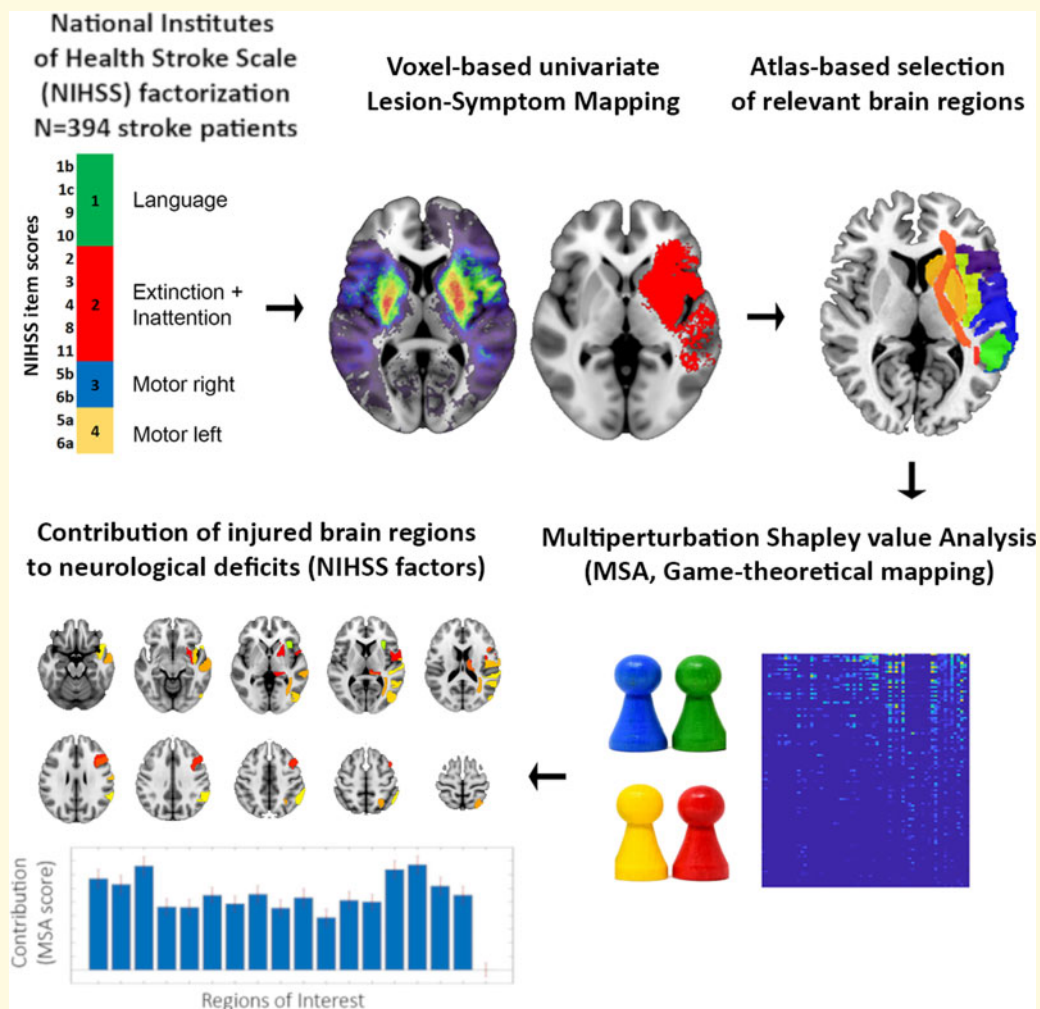
University Medical Center Hamburg-Eppendorf, Martinstraße 52, D-20246 Hamburg, Germany

E-mail: c.malherbe@uke.de

**Keywords:** NIHSS; stroke; multivariate analysis; game theory; lesion inference

**Abbreviations:** FLAIR =FLuid-Attenuation Inversion Recovery; IQR =interquartile range; JHU-ICBM =Johns Hopkins University-International Consortium of Brain Mapping; LSM =lesion symptom mapping; MNI =Montreal Neurological Institute; MSA =Multiperturbation Shapley value Analysis; NIHSS =National Institutes of Health Stroke Scale; ROI =region of interest; RoB =Rest of the Brain; SD =standard deviation; SVM =support vector machine;

## Graphical Abstract



## Introduction

The National Institutes of Health Stroke Scale (NIHSS) is a standardized bedside test designed to assess a broad range of neurological signs in stroke patients. It captures deficits of fundamental brain functions, such as motor functions, speech and spatial attention.<sup>1</sup> The NIHSS is the

most widely used clinical score for quantifying stroke-related clinical deficits in large clinical trials and everyday clinical practice<sup>2</sup> and of high predictive value regarding long-term functional outcome.<sup>3,4</sup> Mapping the contribution of brain lesions to essential clinical phenotypes captured by the NIHSS is, therefore, an important prerequisite for treatment decision making and prognostication in stroke

as well as a valuable approach for systematic inference of fundamental brain functions.<sup>5</sup>

Traditionally, mass-univariate approaches of lesion-symptom inference are of limited sensitivity to anatomical and functional dependencies in stroke lesion distributions and in the functional anatomy of brain regions, which may result in substantially biased inferences.<sup>6,7</sup> Multivariate analyses for lesion-symptom inference which overcome these limitations have emerged in recent years. In particular, Multi-perturbation Shapley value Analysis (MSA), a rigorous multivariate inference method based on game theory, is an innovative and valuable approach for the analysis of behavioural effects resulting from multi-lesion patterns.<sup>8,9</sup> The MSA approach is based on the concept of stroke lesions typically affecting not only one, but several brain regions that contribute and interact in generating a behavioural deficit. Here, brain regions are considered as players of a coalition in a game who interact to achieve a behavioural outcome. Application of MSA is, however, constrained by the large number of datasets ( $2^n$ ) needed to specify or estimate the full range of potential combinations of  $n$  players (or brain regions) and the associated observed outcome (clinical performance). Therefore, a set of brain regions is typically selected *a priori*, potentially limiting the ability to detect relevant contributions of brain areas to clinical performance outside of the initial hypothesis. Moreover, past approaches have often focussed either on contributions of grey matter regions or white matter tracts, but more infrequently on combined grey and white matter contributions.

In our current work, we introduce an innovative three-step approach for applying MSA to a large and representative dataset of patients with acute stroke, in order to reveal the functional contributions of different brain regions to symptom clusters captured by the NIHSS. First, an advanced connectivity-based brain atlas was employed to parcellate the complete grey and white matter at high resolution.<sup>10,11</sup> Second, a mass-univariate lesion-symptom mapping was conducted using a liberal false discovery rate error threshold to pre-identify, or exclude, atlas regions prior to MSA. Third, MSA was applied iteratively to calculate functional contributions of sets of essential atlas regions to clinical performances measured by the NIHSS. We expected these contributions to be lateralized and specific in relation to behavioural domains associated with resulting brain regions.

## Methods

### Sample

We analysed clinical and imaging data from  $N=503$  patients of the WAKE-UP trial, an international, multi-centre (48 sites in 7 European countries), randomized, double-blind, placebo-controlled trial of magnetic resonance imaging (MRI)-based intravenous thrombolysis in patients with unknown onset stroke.<sup>12</sup> Scores of

individual NIHSS items, demographic data (age, sex) and MRI datasets from the time point of admission to the hospital, prior to randomization, were included. Patients or their legal representatives provided written informed consent according to national and local regulations. There was an exception from explicit informed consent in emergency circumstances in some countries.

### Stroke lesion segmentation

To minimize the possible confounding effects based on different sites of acquisition, we have taken a standardized methodology for the stroke lesion segmentation and lesion volumes quantification, as described previously.<sup>13</sup> In summary, all centres applied a standardized protocol including diffusion weighted imaging and Fluid-attenuated inversion recovery (FLAIR) imaging. The WAKE-UP central image reading board continuously monitored the fulfilment of the prespecified MRI standards. Imaging data were analysed by dedicated software developed for the WAKE-UP trial (Stroke Quantification Tool, SONIA) performing registration and semi-automated stroke lesion segmentation based on an apparent diffusion coefficient standardized threshold of  $620 \text{ mm}^2/\text{s}$ , that is commonly used in stroke lesion definitions in clinical routine. After quality control of the segmentation and manual correction where necessary, lesion volumes were calculated on binary lesion maps in native space. Afterwards, lesion masks were transformed to Montreal Neurological Institute (MNI, voxel size:  $1 \text{ mm}^3$ ) space by linear and non-linear registrations based on FLAIR data. FLAIR imaging data were used for registration to the common MNI-space only (and not for lesion delineation). All lesion masks were checked for correct segmentation and registration into MNI-space by two raters experienced in stroke MR imaging (A.K., B.C.). Imaging data with erroneous registration were discarded from analysis.

### Dimensionality reduction of the National Institutes of Health Stroke Scale

Our methodological approach is illustrated in Fig. 1. Clinical deficits were measured using the National Institutes of Health Stroke Scale (NIHSS), which is almost universally applied in large-scale stroke trials and clinical practice for quantifying stroke severity.<sup>14</sup> The NIHSS consists of 15 individual items (Supplementary Table 1) that can be reduced into four main components representing left- and right hemispheric, motor and non-motor brain functions.<sup>1</sup> This underlying factor structure has been validated by dimensionality reduction using principal component analysis.<sup>2</sup> We adopted this four-factor structure as a behavioural performance measure for lesion-deficit mapping, compromising between using the complete NIHSS sum score and all individual items separately. In summary, factor one, referred to in the

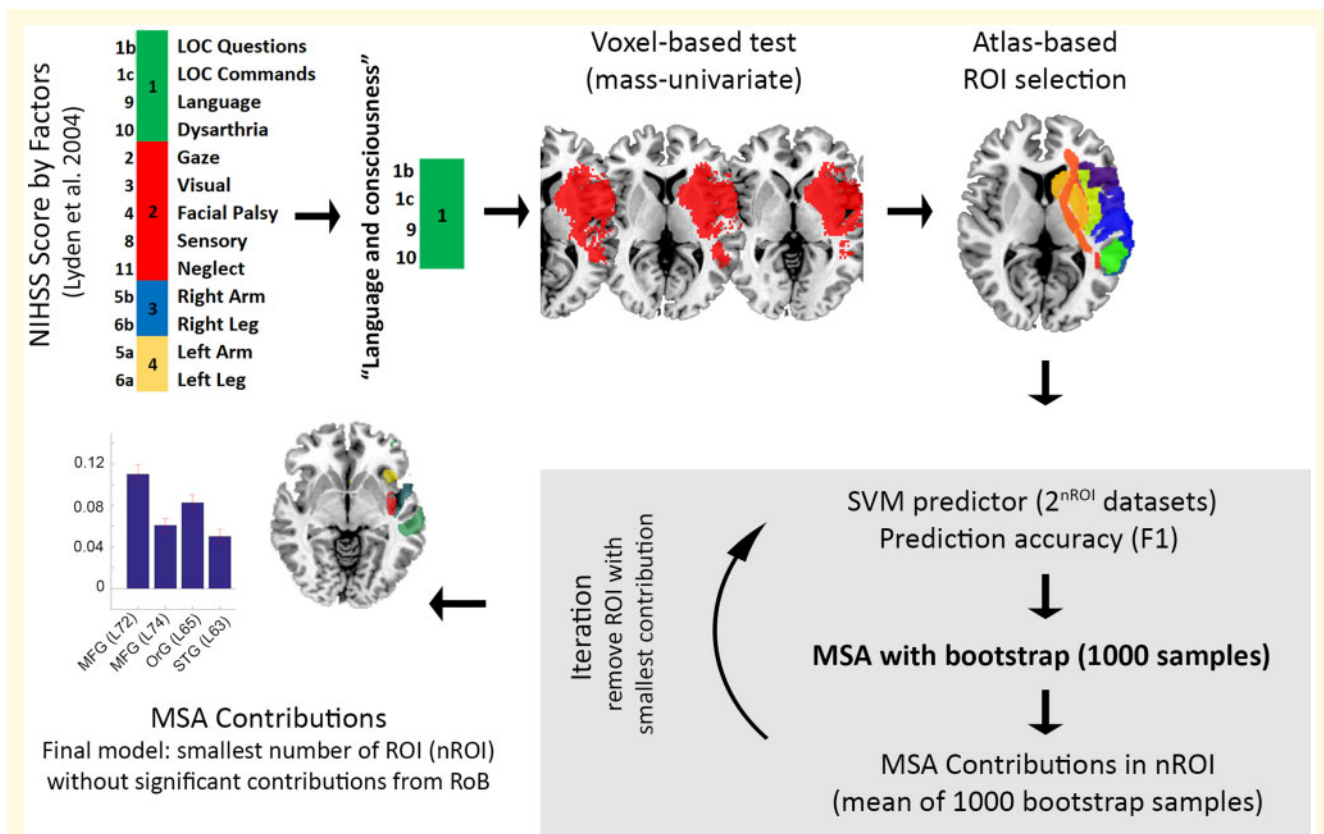


**Figure 1 Methodological approach.** The NIHSS scores were grouped in four factors.<sup>1</sup> For each factor, as for example the ‘language and consciousness’, a mass-univariate LSM was performed on all patients. A grey and white matter atlas was used to label the LSM resulted regions, identifying a set of brain regions. To reduce this set of region to the only one contributing significantly to behaviour, we applied an iterative three-step process (grey box): (i) optimization of SVM for a given database and associated functional performance scores; (ii) computation of an estimated MSA with a bootstrap procedure to ensure the robustness of the results; and (iii) discarding the ROI with the smallest contribution to behaviour and updating the RoB accordingly. These three steps were repeated until the smallest set of ROIs with a non-significant contribution of the RoB. LOC, level of consciousness; nROI, number of Regions of Interest; RoB, Rest of the Brain.

following as ‘language and consciousness’, primarily contains items attributed to left cortical functions (language, level of consciousness questions, level of consciousness commands and dysarthria), factor two, labelled ‘extinction and inattention’, captures functions of the right cerebral cortex (extinction/neglect) and items with bilateral functional representations (such as visual fields), while factors three and four, referred to in the following as ‘right and left motor functions’ contain items pertaining to lateralized motor functions (right arm and leg or left arm and leg). Of note, NIHSS items 1A (level of consciousness) and item 7 (ataxia) are not represented here, due to low contribution to the four-factor structure.<sup>1</sup> The following analysis was conducted separately for each NIHSS factor score, containing the sum of individual NIHSS items grouped as described above.

### Choice of a brain parcellation

Regions of interest (ROIs) comprise the coalition of brain regions with potential contributions to behaviour in MSA

analyses. To ensure sufficient anatomical brain coverage and meaningful interpretability, we defined ROIs based on two anatomical atlases combining white and grey matter, specifically the Brainnetome<sup>10</sup> and Johns Hopkins University-International Consortium of Brain Mapping (JHU-ICBM) atlas.<sup>11</sup> The Brainnetome atlas comprises 246 cortico-subcortical grey matter regions based on the structural and functional connective architecture of the human brain and allows for annotation of behavioural domains. The JHU-ICBM provides labelling for 48 white matter tracts. In cases of overlap between atlases in areas of white matter tracts, labelling from the Brainnetome was preferred, except for the internal capsule, for which the labelling from the JHU-ICBM was chosen. A final ROI representing the rest of the brain (RoB) was created, accounting for stroke lesions affecting other brain region than those predefined by the ROIs in our analysis, in order to avoid significant missing contributions from brain regions not considered in the original composition of ROIs. In total, 295 ROIs were considered for the analysis.



## Statistical analyses

### Pre-selection of ROIs by mass-univariate lesion-symptom mapping

Based on our initial set of 295 ROI, a dataset of  $2^{295}$  cases containing all possible lesion configurations and associated behaviour scores would have to be recorded or estimated for MSA. Since this is an unrealistic scenario even in large-scale stroke imaging datasets, a machine-learning based approach, using a support vector machine (SVM),<sup>15</sup> is applied prior to MSA to estimate the complete set of potential combination of lesion patterns and clinical phenotypes.<sup>16–18</sup> However, given the disproportionately large amount of data ( $n = 2^{295}$ ) that would have to be estimated in the present case, we addressed the problem through reducing the number of regions prior to MSA by computationally feasible mass-univariate lesion symptom mapping (LSM) for each NIHSS factor, to pre-select ROIs potentially involved in lesion-deficit associations. We performed non-parametric mapping implemented in the mricron toolbox (version 2019) with all voxels in bilaterally distributed, binarized lesion masks and NIHSS factor scores.<sup>19</sup> A voxel-wise Brunner–Munzel rank order test (without permutation and without lesion size as covariate), corrected by an intentionally liberal false discovery rate of  $P < 0.05$  was applied. In addition, only resulting clusters with a minimum voxel number of 50 were considered. ROIs were selected for further analysis if they intersected with at least one voxel labelled significant by the mass-univariate statistic.

### Computation of essential ROI sets by iterative MSA

The behavioural database used for MSA computations was derived from the NIHSS factor scores as described above. Since these scores represent the severity of neurological deficit and MSA requires a score representing behavioural ability, we used the inverse of each score as an indicator of functional performance. To compute MSA, the database also included for each patient, the percentage of overlap between the stroke lesions and each ROI.

Following mass-univariate LSM, the number of ROIs was further reduced systematically to identify essential sets of brain regions contributing significantly to behaviour: We applied an iterative three-step process: (i) optimization of SVM for a given database and associated functional performance scores; (ii) computation of an estimated MSA with a bootstrap procedure to ensure the robustness of the results; and (iii) discarding the ROI with the smallest contribution to behaviour and updating the RoB accordingly. These three steps were repeated until the smallest set of ROIs with a non-significant RoB. All steps are described in detail below:

**(1) SVM optimization** In using the SVM approach,<sup>15</sup> the choice of the parameters is crucial. Therefore, we tuned different parameters of the SVM to find the best parameters for the dataset including, for each patient, the

percentage of overlap between stroke lesions and each ROI as well as the associated behaviour. Specifically, the explored parameters were as follows: kernel (Gaussian, linear, polynomial), penalty parameter C (0.1, 1, 10, 50) and gamma (0.001, 0.001, 0.1, 1). All possible combinations of these parameters were tuned for the graded dataset but also with a binarized dataset, which was thresholded by the median value of the percentage of lesioned voxels for each region of interest, as described previously.<sup>18</sup> With each combination of parameters and database, for each NIHSS factor, we applied a ‘leave-one-out’ cross-validation, using in turn each patient from the database as the *validation data* and all the remaining patients as the *training data*. To ensure the quality of the prediction, we compared the true set of performance values of an NIHSS factor with each set of estimated performance values (one for each combination of parameters), by computing the associated F1 score:

$$F1 = \frac{2 * (\text{Precision} * \text{Recall})}{\text{Precision} + \text{Recall}}$$

with  $\text{Precision} = \frac{tp}{tp + fp}$  and  $\text{Recall} = \frac{tp}{tp + fn}$

with tp: true positive, fn: false negative and fp: false positive. The F1 score reaches its best value at 1 (perfect precision and recall) and worst value at 0. Because we used a multi-class SVM, we averaged the F1 score obtained with different cut-off values of the NIHSS factor scores. The F1 score informs on the precision (the ability of the classifier not to label as positive a sample that is negative), and the recall (the ability of the classifier to find all the positive samples). We determined the set of parameters by the one maximizing the quality of prediction, with the highest value of F1.

**(2) Estimated MSA with bootstrap procedure** To quantify causal functional contributions of the ROIs for each NIHSS factor, we used an objective value characterizing the contributions of ROIs across all possible lesion configurations, the Shapley value.<sup>8,20</sup> In this article, we used the estimated MSA to derive the Shapley value. The method has been previously presented in detail.<sup>9,21</sup> The SVM parameters are used in this step to define functional behaviours related to a set of configurations needed in the estimated MSA procedure.

To ensure the robustness of the obtained contributions and to estimate the associated standard error, we performed 1000 samples of bootstrapping the estimated MSA approach with 1000 permutations. Specifically, from the available database, we chose 1000 random samples with replacement, with the size of the original dataset. We then performed the estimated MSA (by the help of the best SVM parameters estimated on the original dataset) on each of these 1000 new bootstrap samples (with the size of the original dataset). Finally, the functional contributions and standard errors of each ROI were averaged across the 1000 samples.

**Table 1 Demographic and imaging characteristics of 394 patients**

Clinical and imaging variable	
Sex (male, percentage)	251 (64%)
Age [years] (mean, SD)	65.9 (10.9)
NIHSS sum score (0–42, median, IQR)	6 (IQR 4–9)
NIHSS factor score 1: language (0–9, median, IQR)	2 (IQR 1–5)
NIHSS factor score 2: right cortex (0–12, median, IQR)	2 (IQR 1–3)
NIHSS factor score 3: right arm & leg (0–8, median, IQR)	1 (IQR 0–4)
NIHSS factor score 4: left arm & leg (0–8, median, IQR)	2 (IQR 1–3.5)
Stroke lesion side (left, percentage)	234 (59.3%)
Lesion volume [ml] (mean, SD; median, IQR)	8.2 (13.5); 2.6 (IQR 0.9–9.5)

IQR, interquartile range; NIHSS, National Institutes of Health Stroke Scale; SD, standard deviation.

(3) **Removing the ROI with the smallest contribution and updating the RoB** From the obtained set of functional contributions, we removed the ROI with the smallest absolute contribution (positive or negative). The number of ROIs was then reduced by one. The RoB was updated accordingly, by adding the discarded ROI, and represented all voxels of the brain not already labelled in the used ROIs. The three steps were repeated until we found the smallest set of regions with a non-significant contribution of the RoB.

### Functional interactions

Additionally, we investigated functional interactions<sup>22</sup> between the regions significantly contributing to each factor. The interaction between two regions quantifies how much the contribution of the two regions considered jointly is larger or smaller than the sum of the contribution of each of them individually when the other one is lesioned. In particular, such interactions can reveal functional redundancies between regions that indicate functional overlap, when the contribution of the joined regions is smaller than the sum of their individual contributions. Alternatively, when the joined contribution is larger than the sum of the individual contributions, the interactions reveal synergistic relations between regions. The interactions were calculated between all significant grey matter regions contributing to an NIHSS factor, extracted by the estimated MSA with bootstrap procedure, for each NIHSS factor. To ensure the robustness of the obtained interactions and to estimate the associated standard error, we performed 1000 samples of bootstrapping the interactions. Specifically, from the available database, we chose 1000 random samples with replacement, with the size of the original dataset. We then calculated the functional interactions for each of these 1000 samples. Finally, the functional interactions and standard errors of each pair of ROIs were averaged across the 1000 samples. We only considered significant interactions

between pairs of ROIs, in the sense that the interaction value should be larger than the standard error.

All analysis was done using in-house scripts (MATLAB, version R2019a, The MathWorks, Natick, MA, USA).

### Data availability

All scripts for the method part are available upon reasonable request. Imaging data from the WAKE-UP-trial are available upon request conditional to approval from the WAKE-UP trial steering committee (<https://www.safe-stroke.eu/wake-up/>).

## Results

Of 503 patients randomized in WAKE-UP, processing of MRI datasets and segmentation of stroke lesion masks was successful in 452 patients, while 51 patients were excluded due to insufficient imaging quality impeding correct delineation or registration of stroke lesions. In addition, patients with bilateral stroke lesions ( $n=17$ ), stroke involving the cerebellum ( $n=7$ ) or the brainstem ( $n=34$ ) were excluded. In total, clinical and imaging datasets from 394 patients {251 males [64%], mean age 65.9 years [standard deviation (SD) 10.9], median NIHSS on admission 6 [IQR 4–9], with IQR: interquartile range} were included for analysis. Demographic and clinical data are presented in Table 1. Median stroke lesion volume was 2.6 ml (IQR 0.9–9.5), and stroke lesions were located in the left hemisphere in 234 (59.3%) patients. Anatomical distribution and frequency of stroke lesions are illustrated in Supplementary Fig. 1.

Results from the initial mass-univariate LSM prior to MSA are illustrated in Supplementary Fig. 2. Out of 295 atlas-based ROI, LSM identified 80 left hemisphere ROI associated with deficits in ‘language and consciousness’, 143 bilateral ROIs with the factor ‘extinction and inattention’, 79 left ROIs with the factor ‘right motor function’ and 64 right ROIs with the factor ‘left motor function’. Supplementary Table 2 lists the individual ROIs subsequently considered in the MSA for each NIHSS component.

The median F1-score of SVM for the NIHSS factor ‘language and consciousness’ was 0.36 (IQR: 0.34–0.37); for factor ‘right motor function’ 0.43 (IQR: 0.42–0.44); for factor ‘left motor function’ 0.49 (IQR: 0.47–0.52). All these values were considerably higher than their corresponding statistical chance levels (0.11; 0.15; 0.16, respectively) computed by using randomly permuted instead of predicted scores. We note that for the factor ‘extinction and inattention’, the F1-score at the first step of the method was 0.1, very close to the F1-score chance level of 0.06. Owing to the limited capability of the SVM parameters to predict this NIHSS factor accurately, we decided to not conduct an MSA analysis for the ‘extinction and inattention’ factor. We speculate that the low performance of SVM results from the broad range of

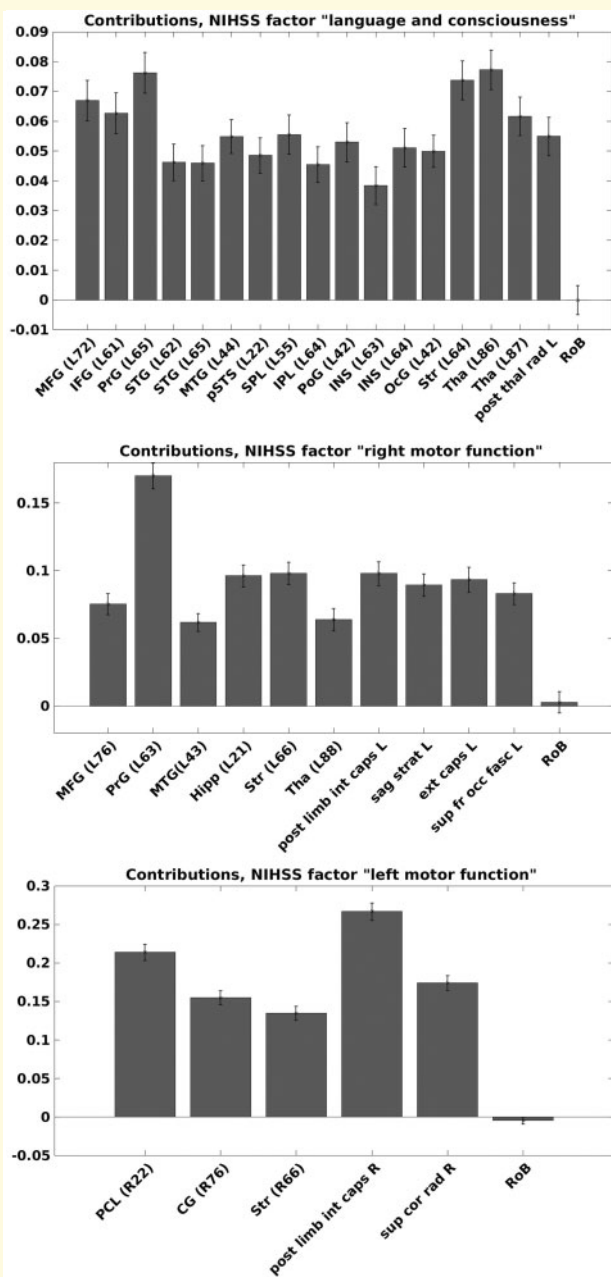


**Figure 2 MSA contributions for each NIHSS factor.** MSA contributions in the last step of the method of NIHSS factors 'language and consciousness', 'right motor function' and 'left motor function'. Normalized mean MSA contribution values and standard deviation (black whiskers) are shown, and derived from the bootstrap procedure with 1000 samples. Positive values indicate that a damage to these brain regions leads to decreased performance in NIHSS factor scores. See Table 2 for abbreviations. RoB, Rest of the Brain.

clinical deficits (extinction, inattention, visual field deficits, sensory functions) grouped into this factor that cannot be related easily to a common combination of injured brain areas. All the parameters from the SVM procedure for the three main functions are listed in

Supplementary Table 3. Nonetheless, we stress that they are specific for a database, the number of considered regions and the associated behaviour.

MSA contribution values were all significantly different from zero, except for the rest of the brain (RoB), where contributions were non-significant according to the standard error calculated by bootstrap analysis. Positive contributions denote that a region facilitates behavioural performance in a given score, as performance decreases if the ROI is lesioned. Detailed results are illustrated in Figs 2 and 3, anatomical regions with significant MSA contributions and associated functional domains are listed in Table 2. In summary, for the NIHSS factor 'language and consciousness', the highest contributions were shown for left hemispheric and predominantly cortical regions of the frontal and temporal lobe. For the NIHSS factor 'right motor function', the highest contributions were identified by MSA for the left precentral gyrus and white matter tracts located in the left internal capsule as well as for the basal ganglia. For the NIHSS factor 'left motor function', white matter tracts located in the right internal capsule and corona radiata showed the highest contributions to clinical performance scores.

We further performed an analysis of functional interactions between grey matter brain regions with significant MSA contributions for NIHSS factor scores 'language and consciousness', 'right motor function' and 'left motor function'. Positive interaction values show that two brain regions jointly contribute more to the measured performance than individually, indicating a synergistic interaction. Functional interactions are illustrated in Fig. 4. In summary for the NIHSS factor 'language and consciousness', highest functional interaction values were observed between the left middle frontal gyrus (inferior frontal junction) and three other regions: the left striatum (ventromedial putamen,  $1.03 \pm 0.79$ ), the left ventral insula ( $1.19 \pm 1.17$ ) and the left inferior parietal lobe ( $1.03 \pm 0.99$ ). We also found high synergistic interactions between the left ventral insula and four regions: the left inferior frontal gyrus ( $0.94 \pm 0.91$ ), the left prefrontal gyrus ( $1.06 \pm 0.72$ ), and two areas of the left superior temporal gyrus, the area 41/42 ( $0.9 \pm 0.65$ ) and the area 38 ( $0.87 \pm 0.57$ ), see Fig. 4 for illustration. No significant interactions between grey matter regions were detected for NIHSS factors 'right motor function' and 'left motor function'.

## Discussion

Our study pursued an innovative, multivariate approach for mapping fundamental brain functions derived from main components of the NIHSS in a large and representative dataset of patients with acute stroke. The analysis yielded two main findings. First, we demonstrated functionally plausible, lateralized contributions of brain regions to individual clinical performance. Second, we revealed synergistic interactions between distinct sets of

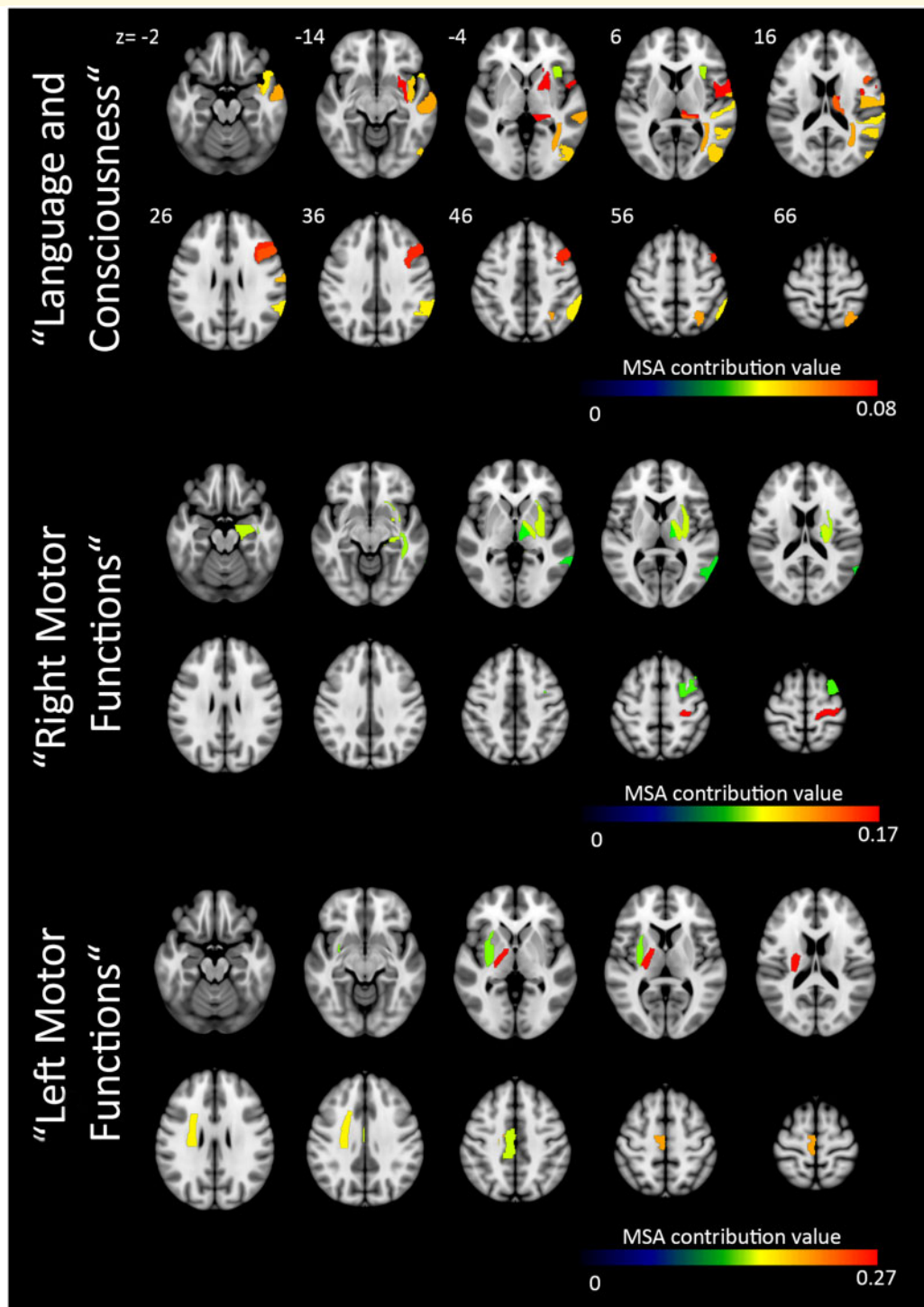


**Figure 3 MSA contributions for each NIHSS factor.** MSA contributions in the last step of the method of each NIHSS factor score in brain regions defined by the Brainnetome and JHU-ICBM white matter tract atlas. Colour bars represent the normalized mean MSA values, the red colour accounting for the highest value, respectively for each factor. Results are illustrated on a brain template in MNI standard space oriented in radiological convention. See also [Table 2](#) for statistical and anatomical details. MNI coordinates of each section (z-axis) are shown.

cortico-subcortical brain regions underlying basic language performance.

Based on the condensed four-factor structure of the NIHSS chosen for our study, the factor ‘language and

consciousness’ comprises NIHSS items ‘language’, ‘dysarthria’ and ‘assessment of level of consciousness’, which in the context of the NIHSS necessitates unimpaired language comprehension and production (patients with



**Table 2 MSA contributions (mean values  $\pm$  SD) in the last step of the method of each NIHSS factor score for grey and white matter regions of the Brainnetome and JHU-ICBM atlas**

Atlas Region	Anatomical description	MSA value	Behavioural domains
<b>NIHSS factor 'language and consciousness'</b>			
MFG L72	Left Middle Frontal Gyrus, inferior frontal junction	0.07 $\pm$ 0.01	Cognition: Language: Phonology and Semantics Cognition: Memory: Explicit and Working
IFG L61	Left Inferior Frontal Gyrus, dorsal area 44	0.06 $\pm$ 0.01	Cognition: Language: Phonology, Semantics, Speech and Syntax Cognition: Memory: Working Action: Execution
PrG L65	Left Prefrontal Gyrus, area 4 (tongue and larynx)	0.08 $\pm$ 0.01	Perception: Somesthesia: Pain Action: Execution: Speech
STG L62 and L65	Left Superior Temporal Gyrus, area 41/42 and Left lateral area 38	0.05 $\pm$ 0.01 0.05 $\pm$ 0.01	Cognition: Language Phonology and Speech
MTG L44	Left Middle Temporal Gyrus, Anterior Superior Temporal Sulcus	0.05 $\pm$ 0.01	Cognition: Language: Phonology, Semantics, Speech and Syntax: Cognition: Memory: Explicit Cognition: SocialCognition Perception: Audition
PSTS L22	Left Caudoposterior Superior Temporal Sulcus	0.05 $\pm$ 0.01	Cognition: Language: Orthography, Semantics, Speech and Syntax Perception: Audition
SPL L55	Left Superior Parietal Lobe, Intraparietal area 7	0.06 $\pm$ 0.01	Cognition: Attention, Reasoning and Space Perception: Vision: Motion
IPL L64	Left Inferior Parietal Lobe, area 40	0.05 $\pm$ 0.01	Cognition: SocialCognition
PoG L42	Left Postcentral Cortex, area 1/2/3 (tongue and larynx)	0.05 $\pm$ 0.01	Action: Execution: Speech Perception: Audition Perception: Somesthesia: Pain Emotion: Disgust Emotion: Fear
INS L63 and L64	Left dorsal agranular Insular and Left ventral granular Insular	0.04 $\pm$ 0.01 0.05 $\pm$ 0.01	Perception: Somesthesia: Pain Emotion: Disgust Emotion: Fear
OcG L42	Left lateral Occipital cortex (V5/MT+)	0.05 $\pm$ 0.01	Perception: Somesthesia: Pain Action: Observation Cognition: Space Interoception: Sexuality Perception: Vision, Motion, Shape Action: Execution Cognition, Emotion
Str L64	Left ventromedial Putamen	0.07 $\pm$ 0.01	–
Thal L86 and L87	Left Occipital Thalamus and Left caudal temporal Thalamus	0.08 $\pm$ 0.01 0.06 $\pm$ 0.01	–
	Left Posterior Thalamic Radiation	0.05 $\pm$ 0.01	–
<b>NIHSS Factor 'right motor function'</b>			
MFG L76	Left Middle Frontal Gyrus, ventrolateral area 6	0.08 $\pm$ 0.01	Action: Execution Action: MotorLearning Cognition: Memory: Working and Space Perception: Vision: Motion
PrG L63	Left Prefrontal Gyrus, area 4 (upper limb)	0.17 $\pm$ 0.01	Action: Execution Perception: Somesthesia
MTG L43	Left Middle Temporal Gyrus, dorsolateral area 37	0.06 $\pm$ 0.01	Cognition: Language: Semantics and Syntax
Hipp L21	Left Hippocampus, rostral	0.1 $\pm$ 0.01	Cognition: Memory: Explicit
Str L66	Left Dorsolateral Putamen	0.1 $\pm$ 0.01	Action: Execution Perception: Somesthesia: Pain
Thal L88	Left Lateral Prefrontal Thalamus	0.06 $\pm$ 0.01	Action: Execution: Speach Perception: Somesthesia: Pain
	Left Internal Capsule, posterior limb	0.09 $\pm$ 0.01	
	Left Sagittal Stratum	0.9 $\pm$ 0.01	
	Left External Capsule	0.09 $\pm$ 0.01	
	Left superior-fronto-occipital Fasciculus	0.08 $\pm$ 0.01	
<b>NIHSS Factor 'left motor function'</b>			
PCL R22	Right Paracentral Lobe, area 4 (lower limb)	0.21 $\pm$ 0.01	Action: Execution Interoception: Bladder Emotion
CG R76	Right Cingulate Gyrus, caudal area 23	0.15 $\pm$ 0.01	
Str R66	Right Dorsolateral Putamen	0.14 $\pm$ 0.01	Action: Execution
	Right Internal Capsule, posterior limb	0.27 $\pm$ 0.01	
	Right Superior Corona Radiata	0.17 $\pm$ 0.01	

Functional annotations of anatomical subregions are given based on behavioural domain meta data labels of the Brainnetome Atlas (<https://atlas.brainnetome.org/brainnetome.html>).

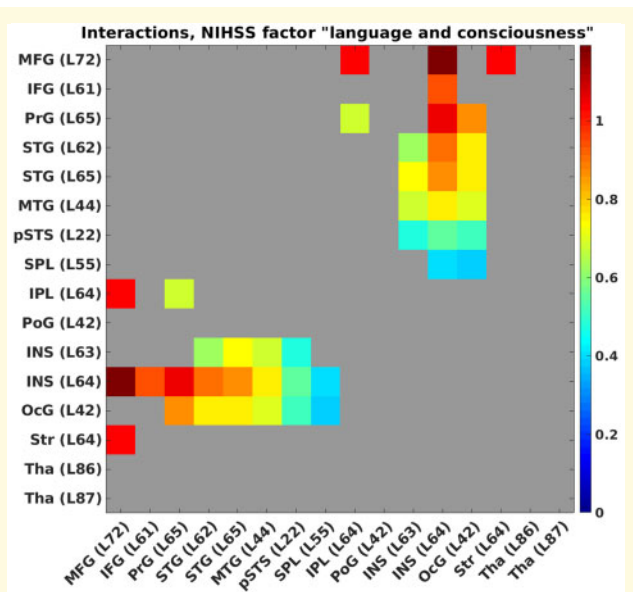


**Figure 4 Functional interactions.** Functional interactions between pairs of regions, for NIHSS factor 'language and consciousness'. The grey colour indicates non-significant results. A positive interaction shows that two brain regions jointly contribute more to the measured performance than individually, indicating a synergistic interaction. See Table 2 for abbreviations.

aphasia are scored with the highest score in item level of consciousness questions). MSA demonstrated strong contributions for a group of left-hemispheric, primarily cortical regions in the frontal, temporal and parietal lobe, such as the middle and inferior frontal gyrus, precentral gyrus, inferior parietal gyrus, middle and superior temporal gyrus (Table 2). Positive MSA contributions indicate that these brain regions facilitate performance in a given task, in line with the known organization of language functions in a left-lateralized, temporo-frontal brain network.<sup>23,24</sup> Strong contributions were also detected for sections of the precentral gyrus (Brodmann area 4) representing the tongue and larynx areas of the cortical motor homunculus. This observation is plausible given the motor component of speech production which, if impaired, results in higher scores on the NIHSS factor. Interestingly, we also observed strong contributions by subcortical grey matter areas, namely the left putamen and thalamus. Although the basal ganglia are traditionally associated with planning and control of motor functions, they are also known to be involved in various aspects of language functions, such as syntactic and speech processes.<sup>25,26</sup> The anterior section of the left putamen was shown to be functionally connected to brain regions involved in language production and comprehension based on a meta-analysis of functional MRI co-activation networks.<sup>27</sup> Similarly, lesions of the left thalamus have shown to be associated with aphasic syndromes, implicating a role of the thalamus in language functions.<sup>28</sup> These observations are in line with the known distribution of language

functions on large-scale brain networks involving cortical and subcortical brain areas.

The NIHSS factors 'right motor function' and 'left motor function' contain test items for rating motor deficits of the right and left extremities. With a total of 16 (8 each) out of 42 possible score points, motor symptoms are represented most prominently in the overall structure of the NIHSS. In contrast to the factor 'language and consciousness', MSA identified mainly white matter tracts and subcortical grey matter areas as main contributors. Specifically, for 'left motor function', the main contributor was the right corticospinal tract as the main efferent pathway of the motor system (Table 2, Fig. 3). These contributions were also seen for the factor 'right motor functions'. In addition, a more complex pattern of regions with positive contributions evolved from MSA for this factor, including the precentral gyrus, specifically primary motor area (Brodmann area 4) and upper limb areas of the motor homunculus. Whereas contributions of the basal ganglia (striatum, putamen and thalamus) would be in line with their known functions in motor control,<sup>29</sup> contributions of the middle frontal gyrus, specifically Brodmann area 6 (Table 2), could indicate an involvement of supplementary motor areas. However, this remains speculative, since the NIHSS does not capture more subtle and complex aspects of motor performance.

For the NIHSS factor 'extinction and inattention', prediction accuracy of the complete configuration of lesion states and corresponding scores by SVM was low and close to results from random shuffling. Therefore, no MSA was conducted for this factor given the expected low validity of resulting contributions. The limited prediction accuracy is most likely explained by the composition of this factor,<sup>2</sup> containing functionally highly heterogeneous NIHSS items (and resulting variance of associated brain areas). Although 'classical' right hemispheric deficits in stroke, such as gaze deviation and extinction/inattention, feature prominently, they appear underrepresented in relation to possible scores from other items with potential bilateral hemispheric representations (facial palsy, sensory deficits and visual fields). In addition, neglect occurs in a significant proportion of left-hemispheric strokes further complicating robust lesion-symptom associations.<sup>30</sup> Therefore, a reliable prediction of associations between brain structure and performance might be unachievable given the lacking specificity of this NIHSS factor. We repeated the analysis of this factor including only NIHSS items 'extinction and inattention' and 'gaze deviation', which did, however, not lead to sufficient prediction accuracy by SVM and significant sets of contributing brain regions (data not shown).

One of the important benefits of using multivariate analysis in lesion inference is that it enables dealing with the fact that stroke lesions typically affect not only one, but several brain regions that contribute to behavioural performance and may be linked functionally as well as anatomically. Univariate approaches are insensitive to the two dimensions of functional and anatomical coupling

regardless of the size of the dataset.<sup>7</sup> By contrast, multivariate approaches such as MSA resolve these problems, depending on the availability of sufficiently extensive and validated clinical datasets.<sup>31</sup> Several positive, functional interactions between lesioned brain areas were shown by MSA in our study, indicating that two brain regions jointly contribute more to a measured performance than individually (Fig. 4), also implying that, if two regions are injured together, the severity of the deficit is increased. For ‘language and consciousness’, the highest synergistic interactions were observed between the left middle frontal gyrus (inferior frontal junction) and the left striatum (ventromedial putamen) as well as the left inferior parietal lobe and the left ventral insula. The left ventral insula was also found for synergistic interactions with four other regions, the left inferior frontal gyrus, the left prefrontal gyrus and two areas of the left superior temporal gyrus (areas 41/42 and 38). We did not find any redundant functional interactions between regions for ‘language and consciousness’. One explanation is that a ‘redundant’ functional interaction between two regions means that they have a similar, partly overlapping. However, the detailed Brainnetome atlas we used to parcellate grey matter brain regions is built to consider regions specific to a function, limiting functional overlap. Moreover, the iterative method used to extract the regions significantly contributing to ‘language and consciousness’ probably already removed all functionally non-essential regions by construction and, in this situation, one should not expect find functional overlaps between two regions. No significant interactions were found for ‘right motor function’ and ‘left motor function’. This would be because the NIHSS does not capture subtle and complex aspects of motor performance, and the primary motor regions are involved alone to the motor function. We should highlight that we only considered grey matter regions for computing interactions because interactions including white matter tracts are challenging to interpret. For example, it is currently unclear how interactions between different white matter tracts should be interpreted; thus, we omitted all white matter tracts from the interaction analysis.

These findings offer insights into the functional brain network organization by highlighting the joint contribution of brain regions to behavioural functions. From a clinical point of view, prognostication of functional outcome after stroke may draw from our findings by acknowledging the disproportionately high impact of damage to synergistic brain regions, guiding individualized rehabilitation efforts.

In this study, we pursued a multi-stage approach with univariate LSM prior to the MSA to pre-select the set of regions. The LSM is a suitable initial step for identifying all potentially involved candidate ROIs, as it yields insensitive but spatially mostly unbiased results in terms of functional anatomy,<sup>7</sup> which findings are subsequently refined and cleared of false positive lesion-deficit

associations by multivariate analysis. Importantly, the initial LSM step allowed us to filter and reduce the number of regions that needed to be considered for the MSA. While, on the one hand, using the entire set of the 295 regions of the atlas would have been the most hypothesis-free approach, it would also have resulted in a computationally impractical strategy, as a space of  $2^{295}$  lesion configurations and associated deficits would need to be considered. Indeed, so far the MSA has been validated for the analysis of up to 100 neural elements.<sup>9</sup> On the other hand, we wanted to avoid the *a priori* selection of a small set of regions for MSA, which would have resulted in a strongly hypothesis-driven approach, producing potentially biasing results by missing contributions from excluded regions or inducing a low interpretability of the results if regions are very large.

Therefore, to pre-select regions by way of the univariate LSM with an intentionally liberal false discovery rate threshold appears to be an acceptable compromise between using the whole set of the 295 regions of the atlas and considering a small set of regions selected *a priori*. As a limitation, it could be argued that our approach using a liberal false discovery rate in mass-univariate testing initially aggravates the number of false-positive results. However, the subsequent iterative multivariate processing with MSA should resolve this problem. To check the validity of our results, we also performed the three steps MSA procedure without the selection of regions by mass-univariate LSM, selecting only regions of the atlas in one hemisphere (the left one for factors ‘language and consciousness’ and ‘right motor function’, the right one for the factor ‘left motor function’). The results (provided in Supplementary Fig. 3) showed similar patterns as what was found in the main analysis. Specifically, the main contributions were made by cortical regions in the temporal and frontal lobe for the factor ‘language and consciousness’; and mainly subcortical regions and white matter tracts for the two motor scores.

In our study, we validated the application of MSA by using a novel using a multi-stage analysis in a large database of stroke patients detecting contributions of brain regions to essential brain functions captured by the NIHSS. We present novel findings of synergistic interactions between brain regions that provide insight into the functional organization of brain networks.

## Supplementary material

Supplementary material is available at *Brain Communications* online.

## Funding

The authors disclosed receipt of the following financial support for the research, authorship and/or publication of

this article: The research leading to these results has received funding from the German Research Foundation (DFG), SFB 936 ‘Multi-site Communication in the Brain’ (Projects A1, C1, C2, Z3) and from the TRR 169 ‘Dynamics of Crossmodal Adaptation’ (Projects A2, A3).

## Competing interests

B.C. reports grants from European Union 7th Framework Program during the conduct of the study and personal fees from Bayer Vital and Abbott, all outside the submitted work. A.K. reports grants from European Union 7th Framework Program during the conduct of the study. M.E. reports grants from European Union 7th Framework Program during the conduct of the study. M.En. reports grants from European Union 7th Framework Program during the conduct of the study, grants from Bayer and fees paid to the Charité from Bayer, Boehringer Ingelheim, BMS/Pfizer, Daiichi Sankyo, Amgen, GlaxoSmithKlineGSK, Sanofi, Covidien, Ever, Novartis, all outside the submitted work. J.B.F. reports grants from European Union 7th Framework Program during the conduct of the study and personal fees from Bioclinica, Artemida, Cerevast, and Nicolab outside the submitted work. I.G. reports grants from European Union 7th Framework Program during the conduct of the study. V.T. reports grants from European Union 7th Framework Program and personal fees and non-financial support from Boehringer Ingelheim, Pfizer/BMS, Bayer, Sygnis, Amgen and Allergan outside the submitted work. K.W.M. reports grants from European Union 7th Framework Program during the conduct of the study, personal fees and non-financial support from Boehringer Ingelheim outside the submitted work. S.P. reports grants from European Union 7th Framework Program during the conduct of the study. C.Z.S. reports grants from Novo Nordisk Foundation and personal fees from Bayer outside the submitted work. C.G. reports from European Union 7th Framework Program during the conduct of the study, personal fees from AMGEN, Bayer Vital, BMS, Boehringer Ingelheim, Sanofi Aventis, Abbott, and Prediction Biosciences outside the submitted work. G.T. reports grants from European Union 7th Framework Program during the conduct of the study, personal fees from Acandis, Boehringer Ingelheim, BMS/Pfizer, Stryker, Daiichi Sankyo, grants and personal fees from Bayer, grants from Corona Foundation, German Innovation Fonds and Else Kroener Fresenius Foundation outside the submitted work. All remaining authors declare no competing interests.

## References

- Lyden P, Claesson L, Havstad S, Ashwood T, Lu M. Factor analysis of the National Institutes of Health Stroke Scale in patients with large strokes. *Arch Neurol*. 2004;61(11):1677–1680.
- Lyden P. Using the National Institutes of Health Stroke Scale: A cautionary tale. *Stroke*. 2017;48(2):513–519.
- König IR, Ziegler A, Bluhmki E, et al. Virtual International Stroke Trials Archive (VISTA) Investigators. Predicting long-term outcome after acute ischemic stroke: a simple index works in patients from controlled clinical trials. *Stroke*. 2008;39(6):1821–1826.
- Yoshimura S, Lindley RI, Carcel C, et al.; for the ENCHANTED Investigators. NIHSS cut point for predicting outcome in supra- vs infratentorial acute ischemic stroke. *Neurology*. 2018;91(18):e1695–e1701.
- Abdul-Rahim AH, Fulton RL, Sucharew H, et al.; VISTA Collaborators. National institutes of health stroke scale item profiles as predictor of patient outcome: external validation on independent trial data. *Stroke*. 2015;46(2):395–400. Epub 2014 Dec 11. Erratum in: *Stroke*. 2015 May;46(5):e128. PMID: 25503546.
- Mah Y-H, Husain M, Rees G, Nachev P. Human brain lesion-deficit inference remapped. *Brain*. 2014;137 (Pt 9):2522–2531.
- Xu T, Jha A, Nachev P. The dimensionalities of lesion-deficit mapping. *Neuropsychologia*. 2018;115:134–141.
- Keinan A, Hilgetag CC, Meilijson I, Ruppin E. Causal localization of neural function: the shapley value method. *Neurocomputing*. 2004;58:215–222.
- Keinan A, Sandbank B, Hilgetag CC, Meilijson I, Ruppin E. Axiomatic scalable neurocontroller analysis via the Shapley value. *Artif Life*. 2006;12(3):333–352.
- Fan L, Li H, Zhuo J, et al. The Human Brainnetome Atlas: A new brain atlas based on connectonal architecture. *Cereb Cortex*. 2016;26(8):3508–3526.
- Hua K, Zhang J, Wakana S, et al. Tract probability maps in stereotaxic spaces: Analysis of white matter anatomy and tract-specific quantification. *Neuroimage*. 2008;39(1):336–347.
- Thomalla G, Simonsen CZ, Boutitie F, et al.; WAKE-UP Investigators. MRI-guided thrombolysis for stroke with unknown time of onset. *N Engl J Med*. 2018;379(7):611–622.
- Cheng B, Boutitie F, Nickel A, et al. Quantitative signal intensity in fluid-attenuated inversion recovery and treatment effect in the WAKE-UP trial. *Stroke*. 2020;51(1):209–215.
- Lyden P, Brott T, Tilley B, et al. Improved reliability of the NIH Stroke Scale using video training. NINDS TPA Stroke Study Group. *Stroke*. 1994;25(11):2220–2226.
- Chang C-C, Lin C-J. LIBSVM: A library for support vector machines. *ACM Trans Intell Syst Technol*. 2011;2(3):1–27:27.
- Malherbe C, Umarova RM, Zavaglia M, et al. Neural correlates of visuospatial bias in patients with left hemisphere stroke: A causal functional contribution analysis based on game theory. *Neuropsychologia*. 2018;115:142–153.
- Zavaglia M, Forkert ND, Cheng B, Gerloff C, Thomalla G, Hilgetag CC. Mapping causal functional contributions derived from the clinical assessment of brain damage after stroke. *Neuroimage Clin*. 2015;9:83–94.
- Zavaglia M, Forkert ND, Cheng B, Gerloff C, Thomalla G, Hilgetag CC. Technical considerations of a game-theoretical approach for lesion symptom mapping. *BMC Neurosci*. 2016;17(1):40. Published online 2016 Jun 27.
- Rorden C, Karnath HO, Bonilha L. Improving lesion-symptom mapping. *J Cogn Neurosci*. 2007;19(7):1081–1088.
- Shapley LS. Stochastic games. *Proc Natl Acad Sci U S A*. 1953;39(10):1095–1100.
- Zavaglia M, Hilgetag CC. Causal functional contributions and interactions in the attention network of the brain: An objective multi-perturbation analysis. *Brain Struct Funct*. 2016;221(5):2553–2568.
- Keinan A, Sandbank B, Hilgetag CC, Meilijson I, Ruppin E. Fair attribution of functional contribution in artificial and biological networks. *Neural Comput*. 2004;16(9):1887–1915.
- Wise RJS. Language systems in normal and aphasic human subjects: Functional imaging studies and inferences from animal studies. *Br Med Bull*. 2003;65:95–119.
- Hickok G, Poeppel D. Dorsal and ventral streams: A framework for understanding aspects of the functional anatomy of language. *Cognition*. 2004;92(1-2):67–99.



25. Teichmann M, Darcy I, Bachoud-Lévi AC, Dupoux E. The role of the striatum in phonological processing: Evidence from early stages of Huntington's disease. *Cortex*. 2009;45(7):839–849.
26. Oberhuber M, Parker Jones O, Hope TM, et al. Functionally distinct contributions of the anterior and posterior putamen during sublexical and lexical reading. *Front Hum Neurosci*. 2013;7:787.
27. Viñas-Guasch N, Wu YJ. The role of the putamen in language: A meta-analytic connectivity modeling study. *Brain Struct Funct*. 2017;222(9):3991–4004.
28. Llano DA. Chapter 9 - The thalamus and language. *Neurobiol Lang*. 2016;95–114.
29. Hening W, Harrington DL, Poizner H. Basal ganglia: Motor functions of. In: MD Binder, N Hirokawa, U Windhorst, eds. *Encyclopedia of neuroscience*. Berlin, Heidelberg: Springer; 2008.
30. Beis JM, Keller C, Morin N, et al.; French Collaborative Study Group on Assessment of Unilateral Neglect (GEREN/GRECO). Right spatial neglect after left hemisphere stroke: qualitative and quantitative study. *Neurology*. 2004;63(9):1600–1605.
31. Toba MN, Malherbe C, Godefroy O, et al. Reply: Inhibition between human brain areas or methodological artefact? *Brain*. 2020; 143(5):e39.